References

ARNDT, U. W. (1978). *J. Phys. E*, **11**, 671-673.
BATTERMAN, B. W. (1978). CHESS Tech. Mem. No. 6.
BECKER, P. & COPPENS, P. (1975). *Acta Cryst.* A**31**, 417-425.
BLESSING, P., COPPENS, P. & BECKER, P. (1974). *J. Appl. Cryst.* **7**, 488-492.
IWATA, M. (1977). *Acta Cryst.* B**33**, 59-69.
IWATA, M. & SAITO, Y. (1973). *Acta Cryst.* B**29**, 822-832.
KVICK, A., MCMULLAN, R. K. & KOETZLE, T. F. (1983). *SYNDAS*. Synchrotron Diffractometer Operating System.
NIELSEN, F., COPPENS, P. & BATTERMAN, B. W. (1984). *ACA Program and Abstracts*, Ser. 2, Vol. 12. Abstract of Annual Meeting, Lexington, KY.
TANAKA, K. (1984). Unpublished results.
TISCHLER, J. Z. (1983). Thesis, Cornell Univ.

Acta Cryst. (1986). B**42**, 364-371

Structural Study of CdY_2S_4

BY A. TOMAS, M. GUITTARD AND J. FLAHAUT

Laboratoire de Chimie Minérale Structurale, associé au CNRS n° 200 (Laboratoire de Physique), Faculté des Sciences Pharmaceutiques et Biologiques, Paris-Luxembourg, 4 avenue de l'Observatoire, 75270 Paris CEDEX 06, France

AND M. GUYMONT, R. PORTIER AND D. GRATIAS

CECM, 15 rue Georges Urbain, 94400 Vitry, France

(*Received* 1 *July* 1985; *accepted* 19 *November* 1985)

Abstract

$M_r = 418{\cdot}46$, cubic, $Fd3m$, $a = 11{\cdot}216\,(3)$ Å, $V = 1411{\cdot}0\,(4)$ Å^3, $Z = 8$, $D_m(293\text{K}) = 3{\cdot}9\,(1)$, $D_x = 3{\cdot}94$ Mg m^{-3}, $\lambda(\text{Mo } K\alpha) = 0{\cdot}71069$ Å, $\mu = 20{\cdot}6$ mm^{-1}, $F(000) = 1400$, $T = 293$ K, $R = 0{\cdot}045$ for 105 independent reflections. The crystal can be described as domains with a disordered rocksalt structure, corresponding to the formula $Cd_2Y_{4/3}S_4$, which grow coherently within ordered domains of spinel structure (98%) of formula CdY_2S_4. In the perturbed NaCl structure, the satellites and linear diffuse streaks along $\langle 111\rangle^*$ are related to substitutive and displacive disorder in the stacking of atomic planes {111}.

1. Introduction

Compounds of formula CdL_2S_4, with L = La–Dy, crystallize in the Th_3P_4 structure or, with a smaller cation radius (L = Ho–Lu and Sc, Y), in the spinel-type structure (Flahaut, Domange & Patrie, 1962; Flahaut, Guittard, Patrie, Pardo, Golabi & Domange, 1965; Flahaut, 1968; Suchow & Stemple, 1963, 1964; Carter, 1972; Tomas, Shilo & Guittard, 1978; Ben Dor & Shilo, 1980). On the basis of a structural determination using an X-ray powder pattern, the ternary sulfide $CdHo_2S_4$ is reported to have a normal spinel structure with a lattice parameter equal to 11·168 Å (Yim, Fan & Stofko, 1973). On the other hand, Fujii (1972) reports the structure of $CdHo_2S_4$, with a cell parameter equal to 11·24 Å, as that of an 'intermediate spinel' with only 60% of the Cd cations occupying the tetrahedral 8(a) positions. This question is clarified by Bakker, Vollebregt & Plug (1982) who have observed the transition from the spinel-type structure to rocksalt structure by electron microscopy and diffraction. These results show that for $T <$ 1173 K, $CdHo_2S_4$ has the spinel structure. For intermediate temperatures, 1173 K $< T <$ 1373 K, the spinel structure becomes unstable, Cd^{2+} shifting from tetrahedral to octahedral positions, and transforms gradually into a rocksalt structure, leading to a transition state. The S lattice is distorted by a planar modulation along (111) and linear diffuse streaks along $\langle 111\rangle^*$ appear in the $(110)^*$ diffraction pattern. In this range of temperature, the crystal is assumed to be built from domains of a NaCl-type structure which grow within a matrix of a spinel-type structure. These features explain the increase of the cell parameter found by Fujii. In the same way, the occupation factor of Cd^{2+} on the tetrahedral site comes from the contribution of spinel domains.

In order to obtain additional information on these questions we have studied the structures of $CdTm_2S_4$, $CdYb_2S_4$ and CdY_2S_4 by means of X-ray diffraction and electron microscopy. The results concerning $CdYb_2S_4$ and $CdTm_2S_4$ are published elsewhere (Tomas, Vovan, Guittard, Flahaut & Guymont, 1985).

2. Experimental

2.1. *Preparation*

Y_2S_3 is prepared by heating the oxide contained in a graphite crucible, using an induction furnace in flowing H_2S. Single crystals of CdY_2S_4 were prepared

0108-7681/86/040364-08$01.50

by heating CdS and Y_2S_3 in stoichiometric amounts in an evacuated quartz ampoule, with KBr, at 1223 K, for one month.

Castaing microprobe analysis, performed on twelve points of one sample, shows two compositions corresponding to CdY_2S_4 and $Cd_2Y_{4/3}S_4$.

2.2. *X-ray diffraction results*

Throughout this paper, indexation of reflections refers to a spinel-type unit cell. Precession photographs of the {110}* pattern show three kinds of diffraction figures (Fig. 1):

(i) Sharp Bragg spots showing the following systematic absences: hkl, $h+k=(2n+1)$ ○; $hk0$, $h+k=2n+1$ ○, which correspond to space group $Fd3m$.

(ii) Satellites arranged in hexagons around Bragg reflections.

(iii) Diffuse streaks along ⟨111⟩* directions (see Figs. 1 and 7*c*).

The satellites have very dissymmetrical intensities which can be classed: $I_1 > I_5 > I_2 > I_4 > I_6 > I_3$. The most intense satellite is always the closest to the centre 000* of the diffraction pattern. The pair (I_1, I_4) is, by far, the most dissymmetrical in intensity, and I_1 and I_4 are far more intense than the corresponding nearest Bragg spot, which is confirmed by microdensitometry. The reciprocal spacing between one satellite and the corresponding Bragg spot is about $\frac{1}{4}$ of the spacing between two Bragg spots along ⟨111⟩* directions. No satellite of higher order than first has been observed.

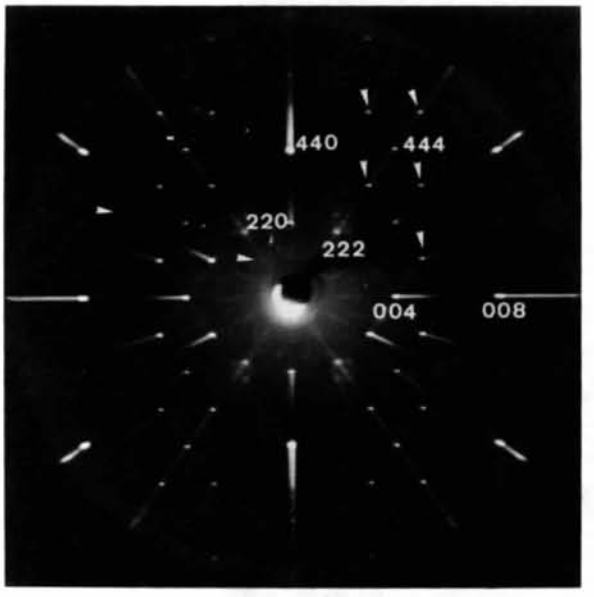

Fig. 1. X-ray precession photograph of a (110) lattice section showing a mixture of NaCl and spinel reflections (spinel reflections are indicated by an arrow). Indices refer to a spinel-type unit cell.

Satellites and streaks appear only in {110}* planes in layer lines 0 and 2.

A crystal of approximately rectangular-prismatic shape (0·009 × 0·007 × 0·006 cm) was measured with a Syntex four-circle automatic diffractometer using Mo $K\alpha$ radiation. A total of 166 intensity measurements ($0<h\leq 9$, $0<k\leq 11$, $0<l\leq 16$) were made up to $2\theta=70°$ with an ω–2θ scan. These reduced to 105 unique reflections with $I>3\sigma(I)$. The cell parameters were refined from the setting angles of 18 reflections in the range $15<2\theta<40°$.

The variation of the standard reflections 400 and 404 was insignificant. The data were corrected for Lorentz and polarization effects. Absorption corrections using the precise shape of the crystal (de Meulaner & Tompa, 1965) were performed by means of the *FACIES* program (Rigoult, Tomas & Guidi Morosini, 1979). The maximum and the minimum absorption corrections are respectively 0·154 and 0·073. The atomic scattering factors and real and imaginary anomalous-dispersion coefficients were taken from *International Tables for X-ray Crystallography* (1974).

The structure was solved using F, with least-squares refinement by *ORFLS* (Busing, 1971); weights = $1/\sigma(F)$. Correction for secondary extinction was insignificant. After refinement, the maximum and minimum heights in the final difference Fourier synthesis were −0·73 and 0·52 e Å^{-3}.

2.3. *Electron microscopy/diffraction* (*see Figs.* 2, 3)

Crystals of CdY_2S_4 were crushed under acetone, then mounted on 400 mesh copper grids coated with thin carbon films. The samples were then examined using a Jeol 200 CX and a Philips EM 300 electron microscope.

The general aspect of the X-ray diffraction patterns is confirmed by electron diffraction. Even the dissymmetrical intensities are clearly visible, in spite of unavoidable dynamical multidiffraction. There is nevertheless important additional information. An exploration of reciprocal space has shown that the structure consists in fact of separated and coherent regions of two different types of structures: a spinel-like structure (Fig. 2), with no diffuse scattering or satellites, *and* a 'perturbed' NaCl-like structure (Fig. 3), giving rise to NaCl-type Bragg spots, plus hexagons of satellites and streaks. Fig. 4 shows a selected-area diffraction pattern taken on a region enclosing both types, quite similar to X-ray precession patterns. Such a mixing of spinel and NaCl types is unavoidable in X-ray diffraction owing to the much less local probing of the X-ray incident beam.

High-resolution images using an objective aperture of diameter 0·05 nm^{-1} were taken with the incident beam along ⟨110⟩.

3. Average structure determination

3.1. *Average structure determination*

The refinement of the structure was started with the atomic positions of the spinel structure, using space group $Fd3m$ and 105 Bragg reflections. The Cd atoms occupy the tetrahedral site $8(a)$; the Y atoms are distributed over the octahedral site $16(d)$ and the S atoms are in $32(e)$ positions. Several cycles of refinement in which the atomic coordinate x of S, the scale factor, the isotropic thermal parameters for all the atoms and the cationic site occupancies were varied, yield an occupancy factor of 0·98 for the $8(a)$ position. The isotropic thermal and occupancy parameters of an atom do not vary in the same cycle and the y and z coordinates of S atoms were constrained to be equal to the x coordinate. The R factor is 0·058. At this point, a difference Fourier synthesis reveals a residual electron density on the $16(c)$ site which is assumed to correspond to an octahedral site of the NaCl-type domains. Referring back to the electron diffraction and microprobe results, a new set of refinements was started supposing that the crystal contains domains with spinel and rocksalt structures; 105 reflections and the space group $Fd3m$ were used. The following assumptions were made:

(i) The crystal contains 98% spinel-type structure [0·98 is the occupation parameter for Cd^{2+} on the

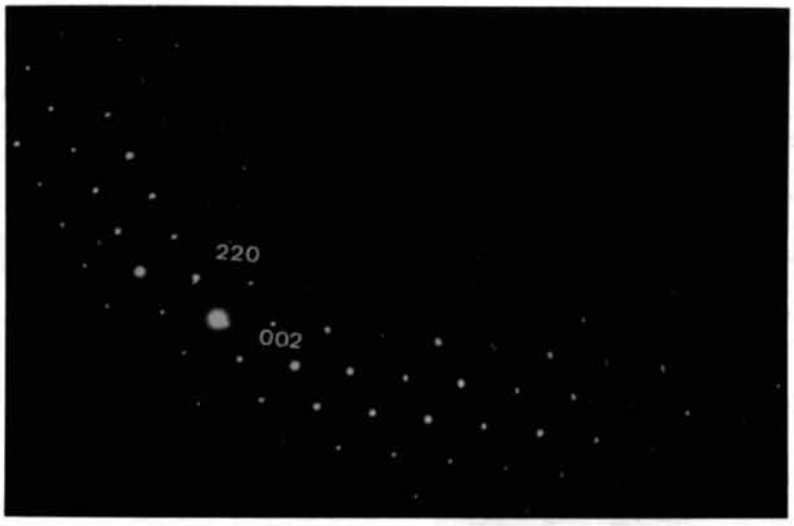

Fig. 2. A (110)* electron diffraction pattern of a spinel-type region.

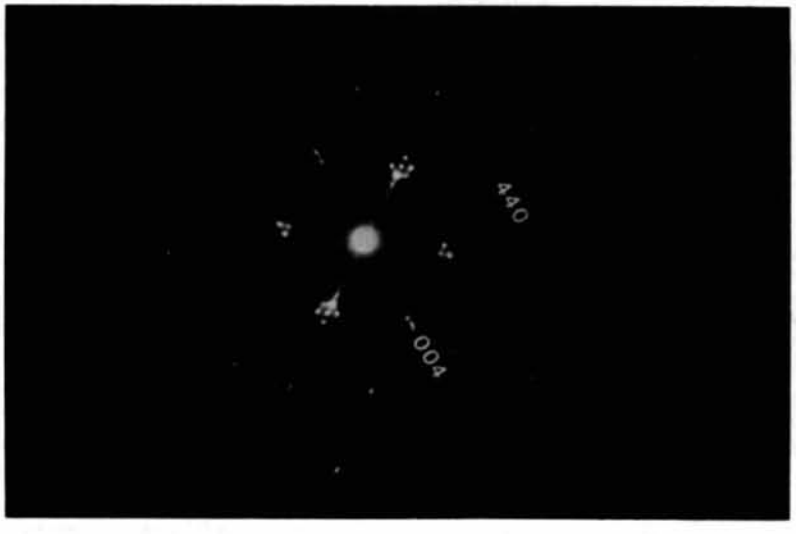

Fig. 3. A (110)* electron diffraction pattern of an NaCl-type region. Indices refer to a spinel-type unit cell. Satellites are clearly visible.

Table 1. *Description of spinel and rocksalt cells*

	Spinel description	NaCl description (I)	NaCl description (II)
Space group	$Fd3m$	$Fd3m$	$Fm3m$
Cell parameter	Contains 8 'CdY_2S_4' a	Contains 8 '$Cd_2Y_{4/3}S_4$' a	Contains 4 $Cd_{1/2}Y_{1/3}S$ $a/2$
S^{2-}	Site 32(e) $x=\frac{1}{4}+\delta$ 0·98 S	Site 32(e) $x=\frac{1}{4}+\delta$ 0·02 S	Site 4(b) 1 S
Tetrahedral position 8(a)	0·98 Cd		
Octahedral position 16(d)	0·98666 Y	0·01 Cd + 0·00666 Y	Site 4(a) $\frac{1}{2}$ Cd + $\frac{1}{3}$Y + $\frac{1}{6}\square$
Octahedral position 16(c)		0·01 Cd + 0·00666 Y	

tetrahedral 8(a) position given by refinement], plus 2% rocksalt-type structure which occurs as domains in the spinel matrix.

(ii) A spinel cell is described with space group $Fd3m$ as indicated in Table 1 and contains eight CdY_2S_4 formula units.

(iii) An NaCl cell is described with space group $Fd3m$ and contains eight $Cd_2Y_{4/3}S_4$ formula units.

With this description the spinel and rocksalt cells have in common the same S lattice described by the 32(e) positions.

0·98 Cd occupies the 8(a) position; (0·098666 Y + 0·01 Cd) and (0·0066 Y + 0·01 Cd) are distributed over the octahedral sites 16(d) and 16(c). The parameters varied are the same as those previously described. The occupation parameters of cations are constrained so as to describe the crystal as built up of 98% spinel structure and 2% rocksalt structure. In order to evaluate the effects of correlations, occupation factors of cationic sites were varied one by one. The deviations of the occupation factors are lower than the standard deviation and the R factor remained constant. The final refinement, with anisotropic temperature parameters, gave $R = 0{\cdot}045$, $wR = 0{\cdot}0525$, $(\Delta/\sigma)_{max} = 0{\cdot}62$.*

Final atomic and thermal parameters and selected interatomic distances are listed in Tables 2 and 3.

In order to improve the final results we attempted a new set of refinements based on:

$$F_{hkl} = \mathrm{Sc} \cdot \left\{ \tau \underset{hkl}{F_1^2} + (1-\tau) \underset{hkl}{F_2^2} + 2\alpha\tau(1-\tau) \underset{hkl}{F_1} \underset{hkl}{F_2} \right\}^{1/2}.$$

Sc is the scale factor, τ the amount (0·98) of spinel cell, F_1 the structure factor of a spinel cell (space group $Fd3m$), F_2 the structure factor of an NaCl cell which is described with space group $Fm3m$ (see Table 1, column 3), and α the degree of coherency between the beams diffracted from the spinel and rocksalt domains.

Different values of α (0 and 1) were tested. The drop in R (0·04) is hardly significant. This is mainly due to the small contribution of rocksalt domains (2%).

4. Discussion

4.1. *Description of the average structure*

These results show that the crystal can be described as domains with the disordered rocksalt structure (2%), corresponding to formula $Cd_2Y_{4/3}S_4$, which grow coherently within ordered domains of spinel

* A list of structure factors has been deposited with the British Library Lending Division as Supplementary Publication No. SUP 42614 (2 pp.). Copies may be obtained through The Executive Secretary, International Union of Crystallography, 5 Abbey Square, Chester CH1 2HU, England.

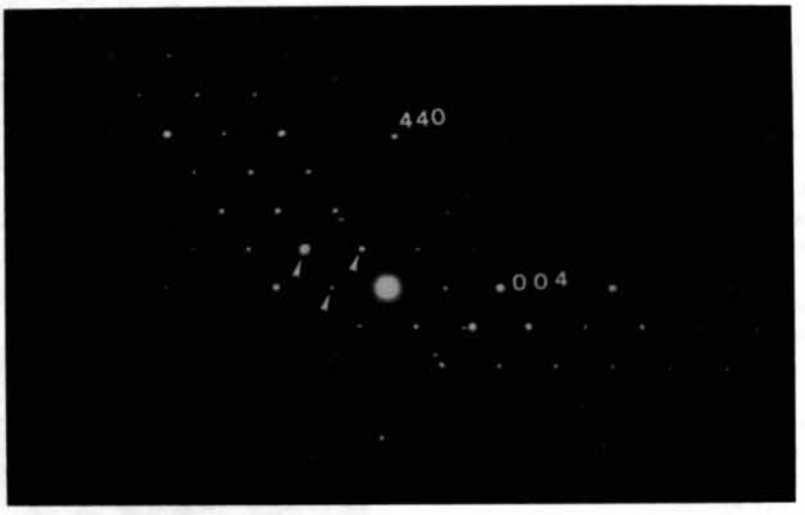

Fig. 4. A (110)* electron diffraction pattern of a region enclosing NaCl- and spinel-type regions. Spinel reflections are indicated by an arrow. Indices refer to a spinel-type unit cell.

Table 2. *Final positional and thermal parameters* ($Å^2$) *for so-called* CdY_2S_4, *with e.s.d.'s in parentheses*

$$B_{eq} = \frac{4}{3} \sum_i \sum_j B_{ij} a_i a_j.$$

Position		x	y	z	B_{eq}
8 (a)	0·98 Cd = Cd (1)	$\frac{1}{8}$	$\frac{1}{8}$	$\frac{1}{8}$	1·54 (13)
16 (d)	0·01 Cd + 0·98666 Y = (Cd,Y) (1)	0	0	$\frac{1}{2}$	1·43 (12)
16 (c)	0·01 Cd + 0·00666 Y = (Cd, Y) (2)	0	0	0	2·04 (19)
32 (e)	1 S (1)	−0·0064 (3)	−0·0064 (3)	−0·2564 (3)	1·30 (18)

Table 3. *Interatomic distances* (Å) *for so-called* CdY_2S_4 *with e.s.d.'s in parentheses*

Position 8(a)		Position 16(d)		Position 16(c)	
Cd(1^i)–S(1^i)	2·553 (6) × 4	(Cd, Y)(1^i)–S(1^i)	2·733 (3) × 6	(Cd, Y)(2^i)–S(1^i)	2·878 (4) × 6
S(1^i)–S(1^{iv})	4·17 (1) × 3	S(1^i)–S(1^v)	3·76 (1)	S(1^i)–S(1^{iv})	4·17 (1)
		S(1^i)–S(1^{ii})	3·968 (1)	S(1^i)–S(1^{iii})	3·968 (1)

Symmetry code: (i) x, y, z; (ii) $-x, y-\frac{1}{4}, z-\frac{1}{4}$; (iii) $\frac{1}{4}+x, -y, \frac{1}{4}+z$; (iv) $x, \frac{1}{4}-y, \frac{1}{4}-z$; (v) $x, -\frac{1}{4}-y, -\frac{1}{4}-z$.

structure (98%) of formula CdY_2S_4. The tetragonal Cd–S distances are in agreement with those found in $CdTm_2S_4$ [2·551 (7) Å] and $CdYb_2S_4$ [2·534 (8) Å] (Tomas *et al.*, 1985). It is notable that the (Cd, Y)–S distance for the octahedral 16(d) site occupied by (0·01 Cd + 0·00666 Y) is slightly shorter than the (Cd,Y)–S distance for the 16(c) site, mainly occupied by the larger Cd cations ($r_{Cd^{2+}} = 0·95$ Å, $r_{Y^{3+}} = 0·892$ Å, $r_{S^{2-}} = 1·84$ Å, Shannon & Prewitt, 1976). The size of the octahedral interstices is determined by the radii of L^{3+}. In the case of CdY_2S_4 or $CdHo_2S_4$ ($r_{Ho^{3+}} = 0·894$ Å) the S lattice can expand locally to accommodate the slightly larger Cd^{2+} which is not possible for $CdTm_2S_4$ ($r_{Tm^{3+}} = 0·869$ Å) and $CdYb_2S_4$ ($r_{Yb^{3+}} = 0·858$ Å) because of the too large difference between the radii of Cd^{2+} and L^{3+} (Tomas *et al.*, 1985).

4.2. *High-resolution electron-microscopy images*

High-resolution images display the same topological feature as a projected potential: electron microscopy is therefore especially powerful in disclosing translation regularities and irregularities (defects). White spots correspond to peaks of electron intensity, and are thus to be correlated with diffracting units repeated by translation.

4.2.1. *High-resolution electron-microscopy images of a spinel-type region.* Fig. 5 (×550 000) was taken on a spinel region: it shows rather perfect regularity indicating an almost ideal structure. A measurement of the periodic spacing along projected {111} gives about 8 Å.

4.2.2. *High-resolution electron microscopy of an* NaCl-*type region.* In contrast, Fig. 6 (×210 000) taken on a NaCl-type region with a relatively low magnification gives the general aspect of this structure. A mesh of lozenge-shaped domains is clearly visible and seems almost regular. In fact, there is only an average regularity, and lozenge boundaries are defect zones, parallel to {111} planes.

Fig. 7(a), taken at a higher magnification, shows more closely the structure of the lozenges. The mesh aspect almost disappears because of sharper details. An average of eight white spots is counted along a projected {111} plane from one lozenge boundary to the next parallel one. A measurement of the spacing between two adjacent white points yields less than 4 Å. This is the distance between two successive {111} planes of S atoms (see Fig. 7). The random (aperiodic) component of the defects arrangement of the NaCl-type structure prevents any computer simulation of contrast. We shall assume that a white spot could be correlated with the diffracting unit $Cd_{1/2}Y_{1/3}S$. Turning to reciprocal space, it is seen that pairs of satellites

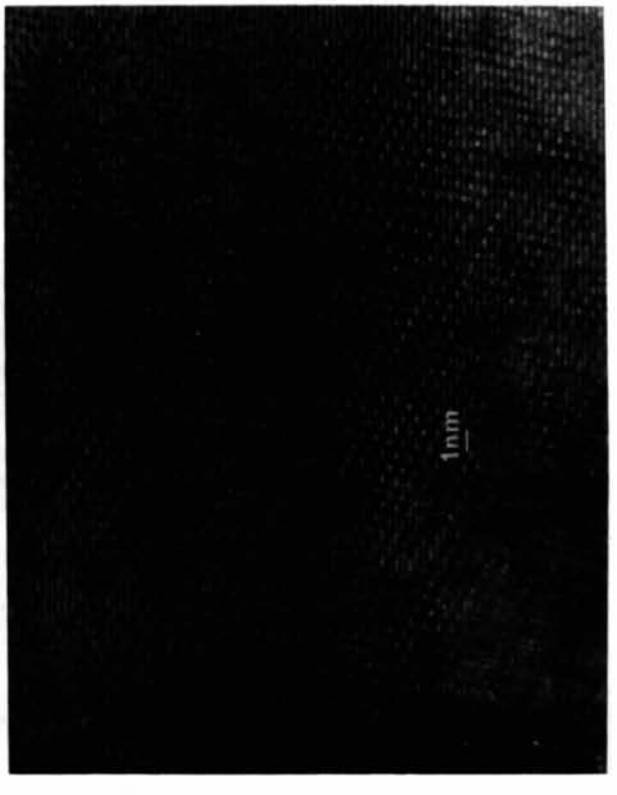

Fig. 5. A (110) high-resolution image of a spinel-type region.

(1, 4) and (2, 5) are correlated with the (almost) regular arrangement of lozenge boundaries; pairs (3, 6), which are less intense, indicate some regularity (on the average) of disturbances in the arrangement of {001} planes (Figs. 7*a*, 7*b* and 7*c*).

A close examination of lozenge boundaries leads to the observation of several features: first, this defect zone is not thin and extends in some places over two or more white spots; thus, the spacing between rows of spots constituting the boundaries seems to be a little larger than the measured interval between two 'normal' white spots; and, last, the contrast between white and dark seems to be greater than outside the boundaries (*i.e.* rows of white spots are more intense and dark spots 'blacker'). All these features contribute to give rise to the lozenge mesh aspect.

Fig. 8 is interesting in that it shows enclosures of the spinel-type structure in a perturbed NaCl-type matrix. These areas are easily located by noting the doubling of the period.

4.3. *Suggested interpretation of satellite distribution intensity*

Unlike the spinel-type structure, which does not raise special problems, the perturbed NaCl-type structure must be considered in detail.

Linear diffuse streaks along ⟨111⟩* are indications of some disorder (substitutive and/or displacive disorder) in the stacking of atomic planes {111}. Satellites, which are far less diffuse, are due, on the contrary, to a periodic order, or, more generally, to the periodic 'component' in the disorder along the

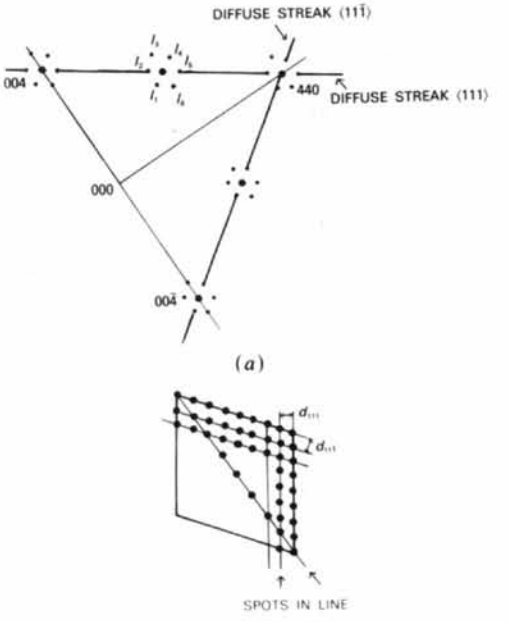

Fig. 6. A (110) high-resolution image of an NaCl-type region showing the general aspect of this structure. A mesh of lozenge-shaped domains is clearly visible.

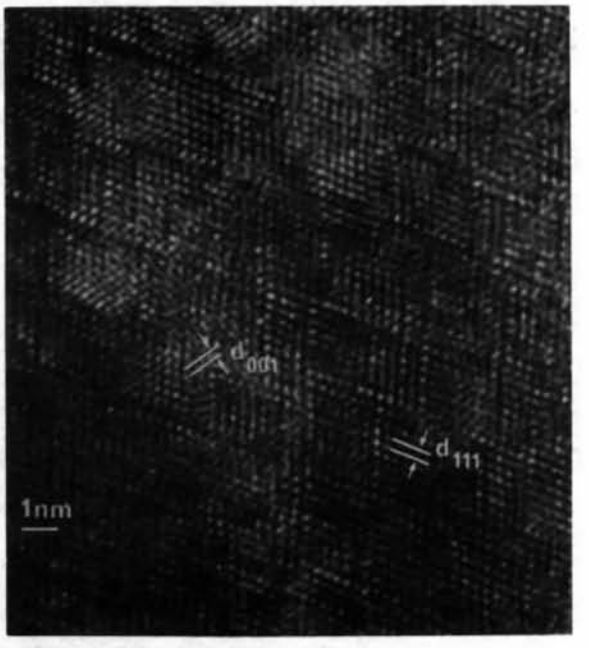

Fig. 7. (*a*) High-resolution image showing the structure of lozenges. A white spot is interpreted as the diffracting unit $Cd_{1/2}Y_{1/3}S$. (*b*) 'Ideal' lozenge whose boundaries are parallel to {111} planes. The spots are in line parallel to {111} and along ⟨001⟩. (*c*) Reciprocal space of (110) corresponding to (*a*).

directions of corresponding pairs of satellites. This latter effect is rendered evident in, for instance, AuCu II (Guymont, Portier & Gratias, 1980). The high-resolution images show that, in this case also, there is only a mean periodic order. Such structures, which are often incommensurate, are called 'statistical structures'.

From a general standpoint, diffraction phenomena realize the harmonic analysis of the structure: the average structure (NaCl) is perturbed by defects and, from the arrangements of these defects, diffraction yields a periodic component (satellites) and an aperiodic (random) component (streaks). In fact, streaks are diffuse (hence aperiodic) along their greatest extensions. In the case of CdY_2S_4, white spots in high-resolution images could be correlated to NaCl-type units (see Fig. 7). Every eight (on the average) NaCl-type units along projection {111}, there is a defect due to displacement and/or substitution in the unit. The mean periodicity leads to the appearance of satellites and the deviation from this mean periodicity gives rise to streaks, more or less diffuse according to the more or less small range of correlation. Furthermore, the strong fluctuation around this mean periodicity is responsible for the extinction of (otherwise possible) higher-order satellites.

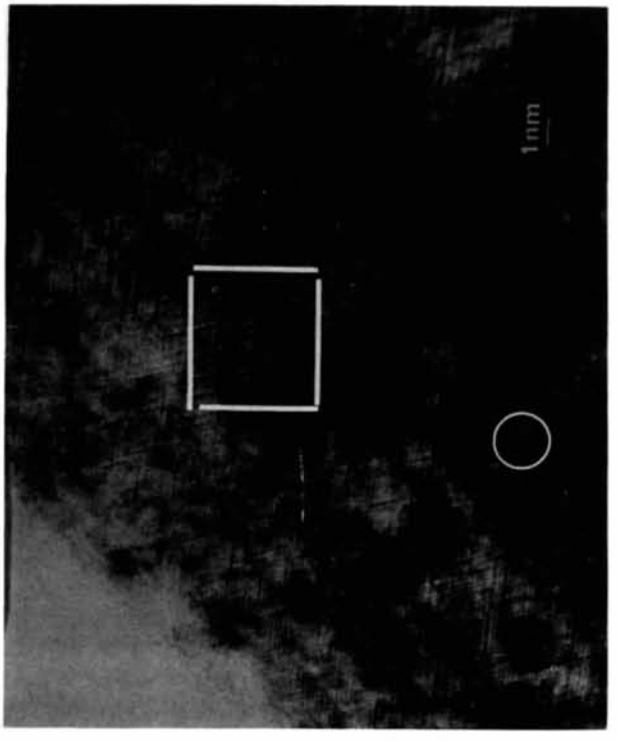

Fig. 8. A (110) high-resolution image showing the enclosures of NaCl-type structure and spinel-type structure. This corresponds to the diffraction pattern of Fig. 4.

On the other hand, the observed dissymmetry in intensity of pairs of satellites is a likely indication of correlation of a (periodic on the average) arrangement of displacive defects with a (periodic on the average) arrangement of substitutive defects. Such a dissymmetry has already been noted in structures such as AuCu II (Jehanno, 1965).

Perturbations of the ideal rocksalt structure described in Table 1 (column 3) should be of two kinds:

(1) '*Substitutive*': The distribution on 4(*a*) of Y^{3+}, Cd^{2+} and the vacancies is not quite stochastic. Four positions of the vacancy are possible per unit of NaCl structure, corresponding to coordinates: $000, 0\frac{1}{2}\frac{1}{2}, \frac{1}{2}0\frac{1}{2}, \frac{1}{2}\frac{1}{2}0$. We suggest that the vacancy lies in one of these four positions for a lozenge with eight (on the average) white-spot sides, then changes position (hence an 'antiphase' defect) and lies in this new position for another eight consecutive lozenges and so on.

To sum up: the perturbed NaCl structure would look like a mosaic of antiphase domains; each are lozenges whose sides are eight (on the average) white spots long.

(2) '*Displacive*': The f.c.c. lattice of S^{2-} undergoes a distortion δ from the coordinate $x=\frac{1}{4}$ of the average structure at each change of position of the vacancy. Note that for most spinel structures, $\delta>0$. Examination of the high-resolution images suggests $\delta>0$, which corresponds to a spreading of {111} planes, thus correlated with the 'substitutive' perturbation of the same (or possibly submultiple) period.

Bakker *et al.* (1982) have reported on $CdHo_2S_4$ electron-microscope observations similar to ours. But these authors did not obtain two separated diffraction patterns corresponding to spinel and perturbed NaCl types. Their study leads to three kinds of diffraction patterns corresponding to three phases of seemingly the same composition: (i) one pattern is associated with an ideal spinel structure ($T<1173$ K); (ii) another pattern corresponds to a rocksalt structure ($T>1373$ K), which we never observed; (iii) and for $1173<T<1373$ K a third pattern corresponding to a 'transition state' which retains (contrary to our case) the sharp spots of the spinel type in addition to a pattern quite similar to that obtained for our perturbed NaCl type. The formation of this 'transition state' is interpreted as due to a migration of Cd^{2+} cations from tetrahedral sites of the spinel-type structure to the octahedral sites, while Ho^{3+} remains in octahedral 16(*d*) sites, and S^{2-} remains in position 32(*e*) with $x\simeq\frac{1}{4}$.

In the case of CdY_2S_4, we agree with the partial ordering of cations, but we cannot consider a regular distortion δ for every {111} plane of S^{2-} because it would lead to the appearance of superlattice spots which we do not observe on electron diffraction pat-

terns. [For instance, the 220 reflection has a structure factor $4f_s(-1+\cos 8\pi\delta)$ which is zero only if $\delta=0$.] Furthermore, in Bakker's model the ordering alone is responsible for the appearance of satellites, and therefore no dissymmetry in intensity is expected.

In conclusion, we propose a model with defects whose substitutive and displacive effects are correlated. These defects form the boundaries of lozenges whose sides are *on the average* eight white spots long. These boundaries are 'thick' {111} planes where there is simultaneously spreading of positions and changes of ordering among possible sites of cations, plus vacancies. The high-resolution electron-microscopy images seem to agree with this model.

A more quantitative interpretation aiming to account for various intensity features (including streaks and dissymmetry of satellites) is in progress. The detailed treatment is not straightforward because of the necessity of taking into account the stochastic components of the arrangement of defects.

References

BAKKER, M., VOLLEBREGT, F. H. A. & PLUG, C. M. (1982). *J. Solid State Chem.* **42**, 11-21.

BEN DOR, L. & SHILO, J. (1980). *J. Solid State Chem.* **35**, 278-285.

BUSING, W. R. (1971). *Acta Cryst.* A**27**, 683-684.

CARTER, F. L. (1972). *J. Solid State Chem.* **5**, 300-313.

FLAHAUT, J. (1968). *Progress in the Science and Technology of the Rare Earths.* Vol. III, edited by L. EYRING, ch. 6, pp. 209-283. Oxford: Pergamon Press.

FLAHAUT, J., DOMANGE, L. & PATRIE, M. (1962). *Bull. Soc. Chim. Fr.* No. 35, pp. 157-159.

FLAHAUT, J., GUITTARD, M., PATRIE, M., PARDO, M. P., GOLABI, S. M. & DOMANGE, L. (1965). *Acta Cryst.* **19**, 14-19.

FUJII, H. (1972). *J. Sci. Hiroshima Univ. Ser A: Math. Phys. Chem.* **36**, 67-75.

GUYMONT, M., PORTIER, R. & GRATIAS, D. (1980). *Acta Cryst.* A**36**, 792-795.

International Tables for X-ray Crystallography. (1974). Vol. IV, pp. 71-78. Birmingham: Kynoch Press. (Present distributor D. Reidel, Dordrecht.)

JEHANNO, G. (1965). Thesis, Univ. of Orsay.

MEULENAER, J. DE & TOMPA, H. (1965). *Acta Cryst.* **19**, 1014-1018.

RIGOULT, J., TOMAS, A. & GUIDI MOROSINI, C. (1979). *Acta Cryst.* B**36**, 1987-1989.

SHANNON, R. D. & PREWITT, C. D. (1976). *Acta Cryst.* A**32**, 751-762.

SUCHOW, L. & STEMPLE, N. R. (1963). *J. Electrochem. Soc.* **110**(7), 766-769.

SUCHOW, L. & STEMPLE, N. R. (1964). *J. Electrochem. Soc.* **111**(2), 191-195.

TOMAS, A., SHILO, I. & GUITTARD, M. (1978). *Mater. Res. Bull.* **13**, 857-859.

TOMAS, A., VOVAN, T., GUITTARD, M., FLAHAUT, J. & GUYMONT, M. (1985). *Mater. Res. Bull.* Submitted.

YIM, W. M., FAN, A. K. & STOFKO, E. J. (1973). *J. Electrochem. Soc.* **120**(3), 441-446.

Acta Cryst. (1986). B**42**, 371-378

Paramètres de Détermination de Structures: Application à Deux Complexes de Type (η_4-Butadiène)tricarbonyle et à Deux Dérivés Cyclohexéniques

PAR J. C. MESSAGER ET L. TOUPET

Groupe de Physique Cristalline, UA au CNRS 040804, *Université de Rennes* I, *Campus de Beaulieu*, 35042 *Rennes CEDEX, France*

(*Reçu le* 20 *mai* 1985, *accepté le* 6 *mars* 1986)

Abstract

A critical study of the automatic resolution of molecular structures by the multisolution method is developed in the particular case of miscrystallized molecular compounds. Some examples are treated to illustrate the choice of 'good information' and how to calculate more precise normalized structure factors and good starting sets. It is shown that it is possible to exclude reflexions at high θ values which can induce false relationships in the convergence process of the tangent formula. Several solutions are proposed which can be used to modify the distribution of the calculated normalized structure factors: over-estimation of the temperature factor, reduction of the resolution sphere, modification of the compound formula, intensities measured at low temperature and critical study of the Patterson function.

Introduction

L'efficacité des méthodes directes de résolution de structure, mises en oeuvre notamment dans le programme *MULTAN*80 (Main, Fiske, Hull, Lessinger, Germain, Declercq & Woolfson, 1980) n'est plus à démontrer.

Des difficultés surgissent cependant, car on sait, par exemple, que certaines structures peuvent présenter des répartitions atomiques très éloignées du

0108-7681/86/040371-08$01.50